# Pathogenesis and treatment of skeletal metastasis : studies in animal models

Buijs, J.T.

# Chapter 3

# Optical imaging of cancer metastasis to bone marrow: *a mouse model of minimal residual disease*

*Am J Pathol* 2002; 160:1143-53

Antoinette Wetterwald [1]
Gabri van der Pluijm [2]
Bianca Sijmons [2]
Jeroen T Buijs [2]
Marcel Karperien [2]
Clemens WGM Löwik [2]
Elsbeth Gautschi [1]
George N Thalmann [1]
Marco G Cecchini [1]

[1] Gene Therapy Laboratory, Department of Clinical Research and Department of Urology, University of Bern, Inselspital, Switzerland

[2] Department of Endocrinology, Leiden University Medical Center, Leiden, Leiden, The Netherlands.

## Abstract

The development of novel anti-cancer strategies requires more sensitive and less invasive methods to detect and monitor *in vivo* minimal residual disease in cancer models. Bone marrow metastases are indirectly detected by radiography as osteolytic and/or osteosclerotic lesions. Marrow micrometastases elude radiographic detection and, therefore, more sensitive methods are needed for their direct identification. Injection of cancer cells into the left cardiac ventricle of mice closely mimics micrometastatic spread. When luciferase-transfected cells are used, whole body bioluminescent reporter imaging (BLI) can detect microscopic bone marrow metastases of ≈0.5 $mm^3$ volume, a size below the limit where tumors need to induce angiogenesis for further growth. This sensitivity translates into early detection of intra-medullary tumor growth, preceding the appearance of a radiologically evident osteolysis by ≈2 weeks. BLI also enables continuous monitoring in the same animal of growth kinetics for each metastatic site and guides end-point analyses specifically to the bones affected by metastatic growth. This model will accelerate the understanding of the molecular events in metastasis and the evaluation of novel therapies aiming at repressing initial stages of metastatic growth.

## Introduction

Because of the progress made in early detection and surgical treatment of the primary tumor, mortality in cancer patients is increasingly linked to metastatic disease. Bone is the second most common site of metastasis [1] and the frequency of bone metastases at autopsy of cancer patients varies between 60 and 85%, depending on the cancer type [2-4].

Clinical and experimental observations indicate that the hematopoietic marrow, rather than the bone tissue, is the initial site of cancer cell seeding [5]. Indeed, small clusters of cancer cells (= micrometastases) can be detected in a vast proportion of the bone marrow aspirates of subjects affected by a variety of epithelial cancers with no radiological or scintigraphic evidence of bone metastasis at the time of diagnosis and/or surgery of the primary tumor [6,7]. Micrometastases represent the pathophysiological basis of minimal residual disease [8,9] (MRD) that will eventually lead to cancer relapse as overt metastases. However, they cannot be detected by conventional staging methods and are poorly influenced by current treatment [8-10]. Hence, there is a need for alternative therapeutic strategies that should be tested in experimental models able to mimic micrometastatic spread.

Injection of cancer cell lines into the left cardiac ventricle of immunodeficient (*nu/nu*) mice is a widely used animal model of bone/bone marrow metastasis [11,12]. This experimental setting closely resembles the clinical situation of MRD after removal of the primary tumor. However, detection of bone metastasis by radiography [13] makes it not an ideal model of MRD. In fact, radiologically evident osteolytic/osteosclerotic metastases are a late and macroscopic event in the evolution of metastatic bone disease. Thus, the model lacks the sensitivity that would be necessary to dissect the initial processes, such as the "angiogenic switch" [14], essential for tumor progression [15]. Furthermore, the radiological detection of osteolytic and/or osteosclerotic metastases is an indirect measure of the tumor burden. Only a parallel histomorphometric analysis allows the distinction between a therapeutic effect exerted directly on tumor cells or indirectly through inhibition of bone resorption. Therefore, more sensitive methods to detect and monitor directly metastatic growth in bone marrow/bone of whole animals need to be developed.

Expression *in vivo* of reporter genes encoding bioluminescent [16] or fluorescent [17] proteins can be detected externally by sensitive detection systems. Cancer cell lines permanently transfected either with the firefly luciferase (*Luc*) or the green fluorescent protein (GFP) have been used to monitor in living mice local tumor growth [18] and development of metastasis to different organs [17].

We investigated the possibility to apply an equivalent bioluminescent imaging method to visualize *in vivo* the development of bone marrow/bone metastases after injection of luciferase-transfected MDA-MB-231 cells, a human mammary carcinoma cell line [19], into the left cardiac ventricle of immunodeficient (*nu/nu*) mice.

Here we demonstrate that whole-body bioluminescent reporter imaging (BLI) effectively allows sensitive localization and growth monitoring of minimal metastatic deposits in the bone marrow at a stage largely preceding tumor-induced osteolysis.

## Materials and Methods

### Animals

Female BALB/c *nu/nu* mice were purchased from Iffa Credo (L'Arbresle, France). They were housed in individual ventilated cages under sterile condition according to the Swiss guidelines for the care and use of laboratory animals. Sterile food and water were provided ad libitum. Mice were 5 to 6 weeks old when used for the intracardiac (i.c.) injection of tumor cells. For intraosseous (i.o.), intra-muscle (i.m.) and subcutaneous (s.c.) implantation of tumor cells they were 10-12 weeks old.

For surgical manipulation, mice were anaesthetized by an intra-peritoneal (i.p.) injection of a mixture of Domitor (1mg/kg body weight; Pfizer, Sandwich, UK), Climasol (10mg/kg body weight; Gräub, Bern, Switzerland) and Fentanyl (100μg/kg body weight; University Hospital pharmacy). Mice were recovered from anaesthesia by a s.c. injection of a mixture of the following antidotes: Antisedan (5mg/kg body weight; Pfizer), Sarmasol (1mg/kg body weight; Gräub) and Narcan (2.4mg/kg body weight; Dupont Pharma, Wilmington, DE).

Mice subjected to i.c. injection of tumor cells were sacrificed by CO2 euthanasia at first signs of distress and/or paraplegia. Mice injected s.c., i.m. and/or i.o. with tumor cells were sacrificed immediately after BLI analysis, and those with tumor cells implanted i.o. were sacrificed at the end of the 5-week observation period.



### Cell lines

The human mammary carcinoma cell line MDA-MB-231 (MDA-231) was obtained from the American Type Culture Collection (Rockville, MD). A sub-clone inducing invariably bone metastases after i.c. inoculation (bone-seeking clone, MDA-231-B) has been established by sequential cycles of i.c. inoculation of MDA-231 *in vivo* and expansion *in vitro* of the cell population recovered from the resulting bone metastases. Briefly, parental MDA-231 cells ($1x10^5$/100 μl PBS) were injected i.c. in female BALB/c *nu/nu* mice. Development of osteolytic bone metastases was monitored by radiography. When the bone metastases reached the size of ≈2 mm diameter, they were dissected out, cut into small fragments and transferred to 12 well-plates. After 3 days of culture, remnants of the original tissue fragments were removed and each area of cell outgrowth was individually trypsinized with the aid of cloning rings. The individual cell populations resulting from each area of outgrowth were separately expanded by limiting dilution. After expansion, the origin of the clones from the cancer cell population of the original metastases was confirmed by species-specific polymerase chain reaction (PCR) analysis for human ß2-microglobulin, as described earlier [20]. Positive clones only were selected for a new

cycle of i.c. inoculation *in vivo* and expansion *in vitro* of the cell population recovered from the resulting bone metastases. The MDA-231-B sub-clone was obtained after a total of four of these consecutive cycles. It showed the capacity, after i.c. inoculation, to induce bone metastases, as detected by radiography, in 100% of the animals. For this reason it was selected for the establishment of stable transfectants expressing the luciferase gene.

Cell lines and the explanted fragments of bone metastases were grown in DMEM Medium (Biochrom, Basel, Switzerland) containing 4.5g glucose/l and supplemented with 10% newborn calf serum (Biowhittaker, Verviers, Belgium) and 1% gentamycin. Cells were regularly certified free of mycoplasma contamination.

### Establishment of stable transfectants expressing the luciferase reporter gene

A CMV-promoter driven mammalian expression vector for luciferase (CMV-Luc) was generated by cloning a full-length firefly luciferase cDNA[21] into the pcDNA3.1 plasmid (Invitrogen, Breda, Netherlands). MDA-231-B cells were transfected with 1 μg CMV-Luc using fugene-6 (Roche Biochemicals, Almere, Netherlands). Stable transfectants were selected with G418 (800ug/ml; Life Technologies, Basel, Switzerland). Twenty-five different G418-resistant clones were isolated, sub-cloned and tested for luciferase activity. Six clones were found to express luciferase activity. One clone (MDA-231-B/Luc+), expressing the highest levels of luciferase activity (5-12 RLU/μg cell protein) was selected for further experimentation. The clone has been cultured up to 40 passages and, even though in some passages the cells have been propagated in absence of G418 selection, the clone maintains currently the same level of luciferase expression of early passages.

### Induction of metastases by intracardiac and intra-venous injection of cancer cells

A single cell suspension of MDA-231-B/Luc+ cells ($1x10^5$/100 μl PBS) was injected into the left heart ventricle according to the method described by Arguello and co-workers.[11] Some animals were injected into the tail vein with an equal number of MDA-231-B/Luc+ cells. The development of metastases was weekly monitored by BLI and radiography. Some of the mice were also imaged 10 minutes and 24 hours after i.c. injection to visualize the early body distribution of MDA-231-B/Luc+cells.

### Intraosseous implantation of cancer cells

For direct i.o. implantation of MDA-231-B/Luc+ cells, two holes, distant 4-5 mm from each other and each with a diameter of about 0.35 mm, were drilled through the bone cortex of the upper third of the right tibia with the aid of a dental drill (Hedstroem file, 28mm/30; Maillefer Instruments, Ballaigues, Switzerland). Space in the marrow cavity was created by flushing out the bone marrow of the proximal segment of the bone shaft. The upper hole was sealed by surgical bone wax (Ethicon, Johnson & Johnson, Somerville, NJ) and a single cell suspension of MDA-231-B/Luc+ cells ($1x10^4$/2 μl of PBS) slowly inoculated via a 30-gauge

needle inserted through the lower hole. Finally, the lower hole was sealed with surgical bone wax and the cutaneous wound was sutured. Local tumor development was monitored twice a week by BLI and radiography. This method was adopted to prevent spill of cancer cells from the channel created by the needle and subsequent growth outside the marrow cavity into the surrounding soft tissues during the following period (28 days) of monitoring.

### Determination of the lowest cell number detectable in bone

The knee articulation was forced in a flexed position and a 27-gauge needle was inserted through the patellar tendon and guided toward the articular surface of the femur with gentle drilling motion until the bone cortex was perforated.[22] Ten thousand to 1 million MDA-231-B/Luc+ cells in a total volume of 5 μl of PBS were slowly injected into the bone marrow cavity. As control, 1 x $10^4$ cells were injected i.m., in the vastus lateralis. As further control, 1 x $10^1$, 1 x $10^2$, 1 x $10^3$ and 1 x $10^4$ cells were injected s.c., in the ventral region. A single BLI analysis was performed after 15 minutes. The choice of this less invasive and faster method of cell inoculation was essentially dictated by the necessity to detect bioluminescent emission immediately after cell implantation and by the fact that in this case spill of cancer cells into the soft tissue was less an issue since tumor growth was not followed up.

### Bioluminescent reporter imaging (BLI)

An imaging system essentially equivalent to that described by Contag and co-workers [18] was used. The imaging unit consists of an intensified charge-coupled device (CCD)-camera (VIM camera, model C2400-47, Hamamatsu Photonics, Hamamatsu, Japan) fitted to a light-tight chamber (Hamamatsu Photonics) and equipped with a 50 mm/f 1.2 Nikkor lens (Nikon, Küsnacht, Switzerland). The images are generated on an Argus-20 image processor (Hamamatsu Photonics) and transferred via SCSI using a software module (Open*lab*™, Improvision, Coventry, UK) to a computer (Macintosh G4, Apple Computer, Cupertino, CA) and processed by an image analysis software (Open*lab*™, Improvision, Coventry, UK).

For the detection of luciferase expressing cells, mice were anaesthetized as described above, but using half the doses of each sedative. Thirty μl of a 250 mM aqueous solution of luciferin (D-Luciferin Na salt; Molecular Probes, Leiden, Netherlands) were injected i.p. 15 minutes before beginning photon recording. Mice were placed in the light-tight chamber and a grey-scale image of the animal was first recorded with dimmed light. Photon emission was then integrated over a period of 5 minutes and recorded as pseudo-color images. For co-localization of the bioluminescent photon emission on the animal body, grey-scale and pseudo-color images were merged by using the Open*lab*™ imaging software.

### Quantification of the bioluminescent signal

The bioluminescent signal was quantified by measuring the amount of highlighted pixels in the area shaped around each site of photon emission with the aid of the Openlab™ imaging software.

### Detection of bone lesions by radiography

Radiographs of the mice, anaesthetized as described above for the BLI analysis, were taken using X-Omat TL films (Kodak, Lausanne, Switzerland).

### Immunohistochemistry

The mice injected i.c. MDA-231-B/Luc+ cells were perfused, after sacrifice, with 60 ml of HBSS containing 20U heparin/ml and, then, with 100 ml of 4% paraformaldehyde in Dulbecco's PBS, pH 7.4. Bones that were shown by BLI to be site of bioluminescent emission were selectively excised and further fixed overnight by immersion in fixative at 4°C. After decalcification in EDTA they were processed for paraffin embedding.

Five µm serial sections, after re-hydration and endogenous peroxidase block, were digested for 20 minutes at 37°C with trypsin (0.1% in 25mM Tris, 140 mM NaCl and 10mM CaCl2) for antigen retrieval. Rabbit antibodies (10 µg/ml) against human pan-cytokeratin (Dako, Zug, Switzerland) or control normal rabbit IgG (Jackson ImmunoResearch, La Roche, Switzerland) were followed by biotinylated swine anti-rabbit Ig antibodies (Dako) and streptavidin-biotinylated peroxidase complex (Amersham, Dubendorf, Switzerland). The reaction was developed with 3- amino-9-ethyl-carbazole as chromogen. Sections were slightly counter-stained with hematoxylin. Size measurements of metastatic lesions were performed with the aid of an image analysis software (NIH Image; http://rsb.info.nih.gov/nih-image).

## Results

### Monitoring in vivo development of metastases after intracardiac and intra-venous injection of cancer cells

In general, within 2 hours from the intracardiac injection of MDA-231-B/Luc+ cells 14 % of the mice died or showed signs of distress, for which they were subjected to euthanasia. The surviving mice all developed bone metastases, as detected by BLI. In contrast, none of the mice ($n$ = 4) injected intra-venously showed either bone or soft tissue metastases during the entire period of observation (4 weeks), as detected both by BLI and radiography.

Ten minutes after i.c. injection of MDA-231-B/Luc+ cells, BLI showed diffuse photon accumulation over the entire animal body, with exclusion of the distal fore- and hind-legs, and of the tail (Fig. 1*A*). Twenty-four hours later photon emission from the same animal was abolished (Fig. 1*B*). However, after 4 weeks BLI could detect distinct areas of photon accumulation, suggestive of metastatic tumor growth, over the hind-legs and over the maxillo-facial region of the same animal (Fig. 1*C*).

First evidence of bioluminescent emission from bones, indicative of bone metastasis, was seen at day 24 after i.c. injection of cancer cells. In all mice ($n$ = 4) discrete photon accumulation was localized over the distal metaphyses of the femurs (Fig. 2*A-D*) and over the

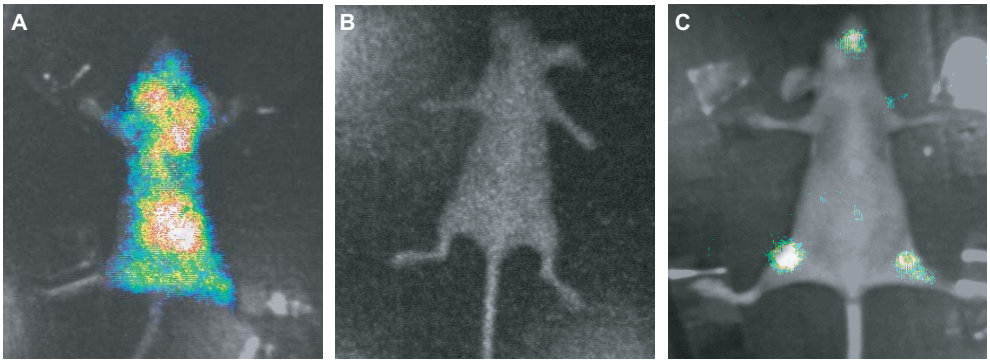


**Figure 1** **Fate of MDA-231-B/Luc+ cells injected into the left cardiac ventricle**. Bioluminescent photon emission was externally imaged from the ventral projection of the same mouse 10 minutes (*A*), 24 hours (*B*) and 28 days (*C*) after injection. Signals are displayed as pseudo-color image (blue least intense, white most intense) at a 0-4 bit sensitivity range merged with the gray-scale body image of the mouse.

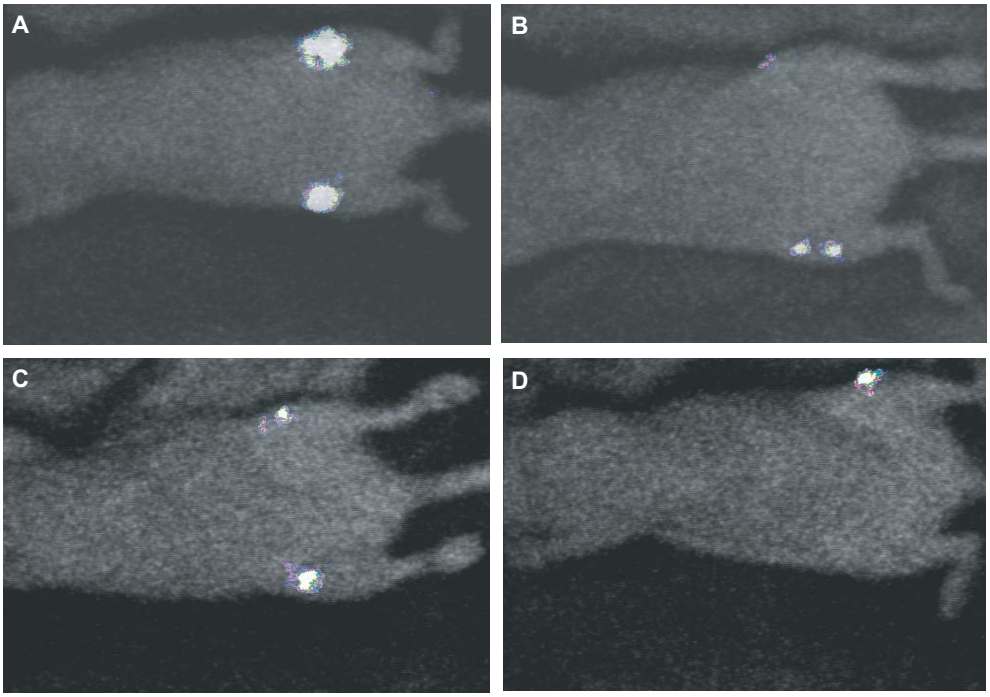


**Figure 2** **BLI monitoring *in vivo* the kinetics of bone metastatic growth**. Bioluminescent photon emission was externally imaged 24 days after injection of MDA-231-B/Luc+ cells into the left cardiac ventricle. *A-D*, ventral projections of four different mice. Signals are displayed as pseudo-color image at the most sensitive 0-3 bit range.

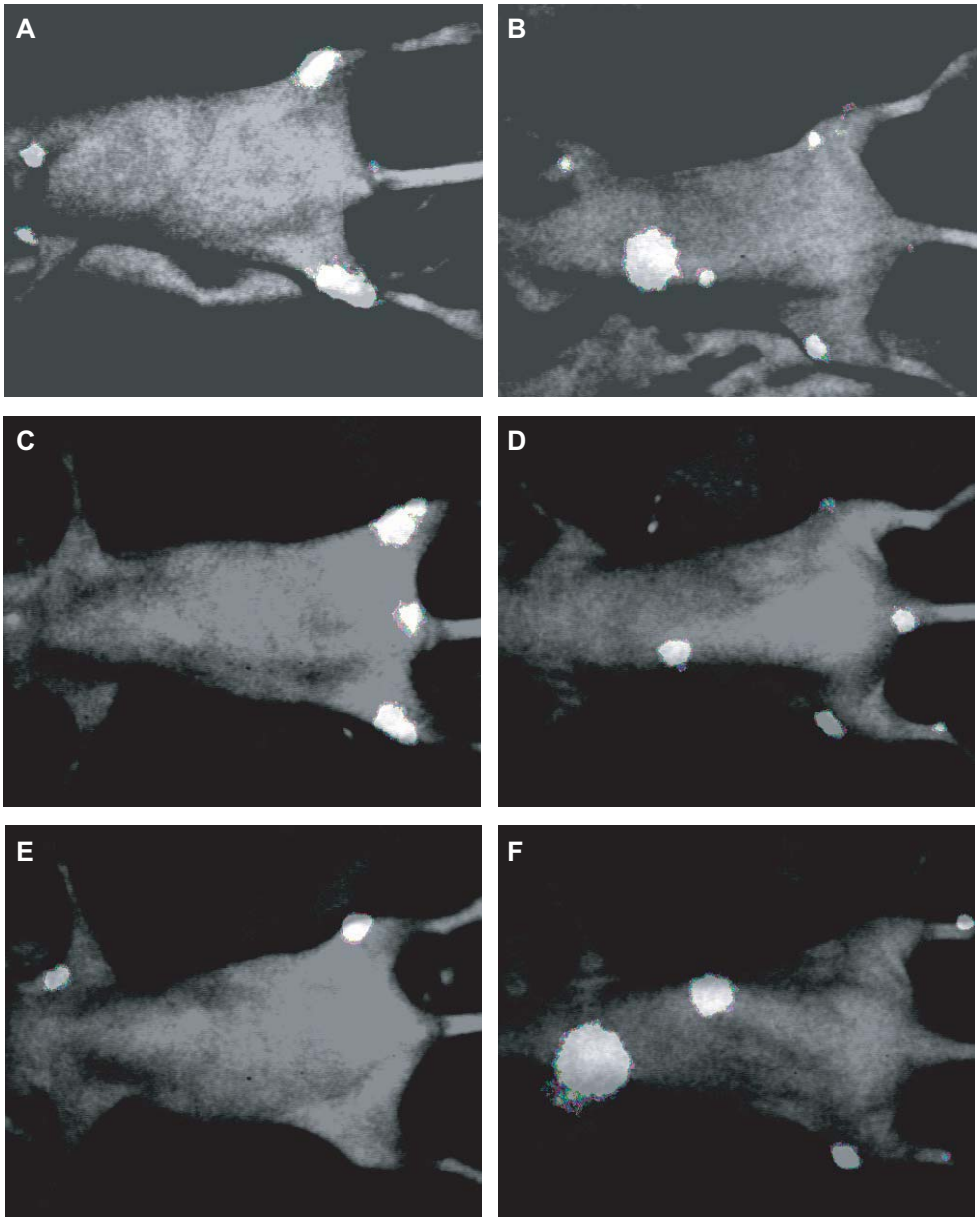


**Figure 3** **BLI monitoring *in vivo* the kinetics of bone metastatic growth**. Bioluminescent photon emission was externally imaged 33 days after injection of MDA-231-B/Luc+cells into the left cardiac ventricle. Ventral (*A, C, E*) and dorsal (*B, D, F*) projections of the three mice shown in panels *B, C*, and *D*, respectively, of figure 2. Signals are displayed as pseudo-color image at a 0-5 bit range, less sensitive than that of figure 2, to optimize the anatomical localization.

dorsal projection of the thoracic vertebrae (not shown). In one mouse photons accumulated also over the proximal metaphysis of the tibia (Fig. 2*B*). Whole body radiographs taken at day 25 did not show any sign of osteolysis in any of the bones and, more specifically, in any of the bone locations that were origin of photon emission recorded the previous day (not shown).

The intensity of photon emission at the bone sites described above increased substantially from day 24 to day 33. Furthermore, at day 33, additional bone sites of bioluminescence became apparent (Fig. 3*A-F*). At this time point, the average number of bone metastasis/mouse attained to 6.33 (± 1.45, SEM). However, whole body radiographs taken at the same day showed bone lesions only in 1/3 of the bone sites revealed by photon detection (total 19 versus 6 bone sites, as detected by BLI and radiography, respectively; *n* mice = 3) (not shown). One animal survived until day 38 after i.c. injection of cancer cells. In this mouse an additional bioluminescent site appeared in the region of the sacral vertebrae (Fig. 4*B*). Meanwhile, the signal intensity over all the other bone sites further increased (Fig. 4*A-C*), as compared to day 33. However, the radiographic analysis of the bone lesions at day 38 did not reveal a modification in their number (Fig. 4*D*), as compared to day 33. In all cases the bone lesions were characterized by subtle modifications of the metaphyseal spongiosa due to increased bone remodeling and/or limited areas of osteolysis (Fig. 4*E,F*). At any time point, none of the animals of this series did show photon emission at extra-skeletal locations.

The quantification of the bioluminescent signal localized over the different bone metastatic sites from the time of their first appearance to the time of animal sacrifice (Fig. 4*G*) allowed continuous monitoring *in vivo* of the growth kinetics for each single bone lesion.

Immunohistochemical analysis for human pan-cytokeratin expression confirmed the presence of cancer cells in all the bones that were shown by BLI to be site of bioluminescent emission. One bone metastatic growth was identified both by BLI and radiography as located in the proximal metaphysis of the humerus (Fig. 4*A,D*). The histological and immunohistological analyses showed that cancer cells have extensively invaded the proximal half of the bone marrow cavity of this bone (Fig. 5*A,C*). In contrast, small bone metastases were apparently located by BLI on the distal region of both tibiae (Fig. 3*D,F* and Fig. 4*A-C*), but their presence was not corroborated by radiological signs of increased bone turnover located in the same or in neighboring bones. However, the histological and immunohistochemical analysis of the bones in this region revealed that a single metastatic focus was located in the epiphysis of each calcaneus bone (Fig. 5*B,D*).

MDA-231-B/Luc+ cells were i.c. injected in another series of mice (*n* = 12) to further investigate the potential of this specific bone-seeking clone to metastasize to organs other than bone and to demonstrate the ability of BLI to detect development of soft tissue metastasis. Bone metastases developed in 100% of the mice (12/12; average number of bone metastases/mouse: 5.33 ± 0.78 SEM). Soft tissue metastases were detected by BLI in 33 % of the mice (4/12; average number of soft tissue metastases/mouse: 0.33 ± 0.14 SEM). Lung and brain were the organs affected by the metastatic process in 25% (3/12) and 8% (1/12), respectively, of the mice injected.

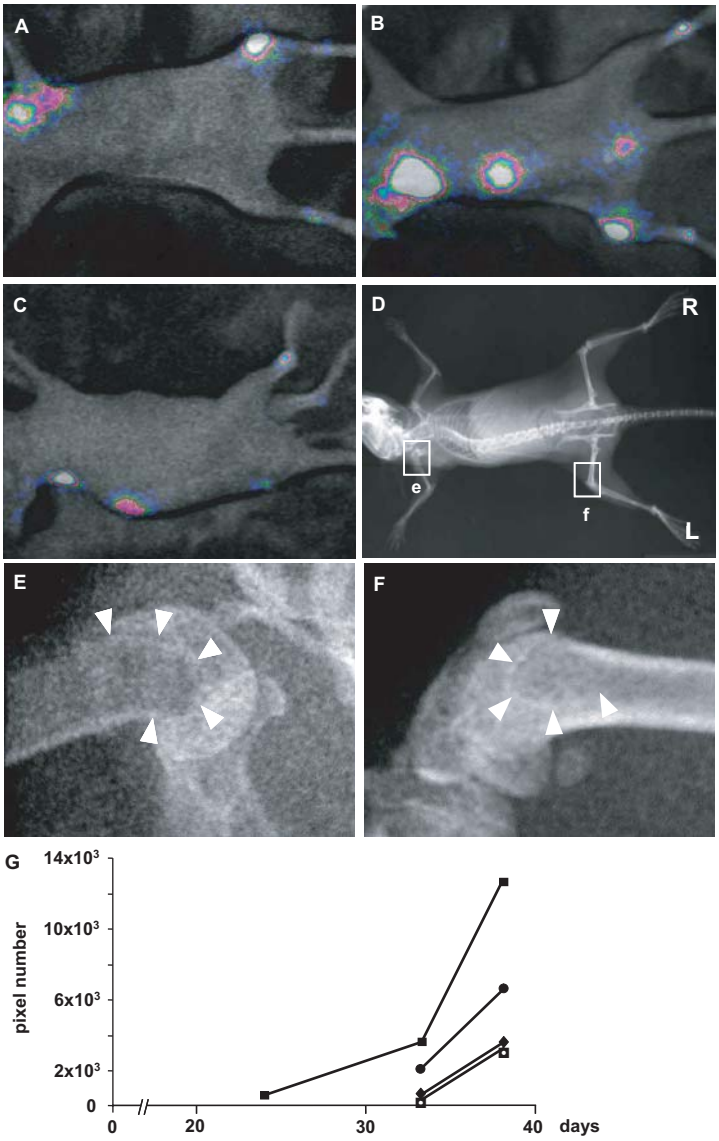


**Figure 4** BLI and radiographic monitoring in vivo the kinetics of bone metastatic growth. Bioluminescent photon emission was externally imaged 38 days after injection of MDA-231-B/Luc+ cells into the left cardiac ventricle. Ventral (*A*), dorsal (*B*), and lateral (*C*) projections of the mouse shown in panels E and F of figure 3. Signals are displayed as pseudo-color image at a 0-6 bit range, less sensitive than that of figure 4, to optimize anatomical localization. *D*, whole body radiograph. R = right side, and L = left side of the mouse. The two regions delimited by the rectangular frames (E) on the proximal humerus and (F) on the distal femur are magnified in (*E*) and (*F*), respectively, showing details of the bone density. Arrowheads point at osteosclerotic rims delineating areas of discrete osteolysis. *G*, growth curve obtained by quantification in the same mouse of the bioluminescent signal localized over the left femur(■) at day 24, as shown in figure 2, D, and over the central portion of the spine (●) and the distal regions of the right (◆) and left (◘) tibia at day 33, as shown in figure 3, E and F, and at day 38 (*A, B*).

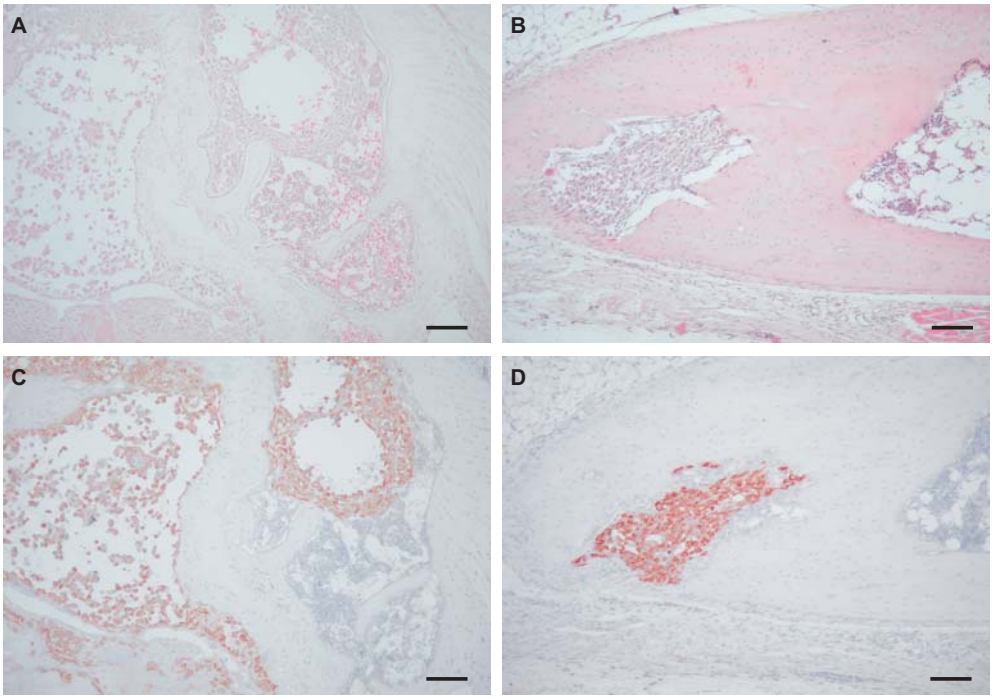


**Figure 5** **Histological and immunohistological identification of MDA-231-B/Luc+ cells in two representative sites of metastasis**. Hematoxylin-eosin staining of sections from the left humerus (*A*) and the left calcaneus (*B*). Cytokeratin immunohistochemistry of adjacent sections from the same humerus (*C*) and calcaneus (*D*). Cells immuno-reactive with the anti-human pan-cytokeratin antibody are stained in brownish-red. Bars represent 100 μm.



During the entire experimental period in both series of i.c. inoculated mice none of the bone metastases detected by BLI showed a decline in bioluminescent activity. Furthermore, conventional radiography never detected an osteolytic lesion not showing bioluminescent emission.

## Monitoring in vivo tumor growth after intraosseous implantation of cancer cells

Soon after implantation of $1x10^4$ MDA-231-B/Luc+ cells into the tibia marrow cavity, no bioluminescent emission could be detected externally. However, already after 4 days there was a defined, although weak, photon emission localized over the area of implant. The signal on the same area increased progressively and became intense from day 14 (Fig. 6*A*). Nevertheless, radiographs taken at equivalent time points (Fig. 6*B*) showed initial signs of osteolysis only at day 14. The osteolysis in the trabecular bone became clearly evident at day 25, and substantial erosion of the cortical bone was obvious at day 36.

The quantification at different time points of the bioluminescent signal localized over the site of implantation (Fig. 6*C*) allowed continuous monitoring *in vivo* of tumor growth.

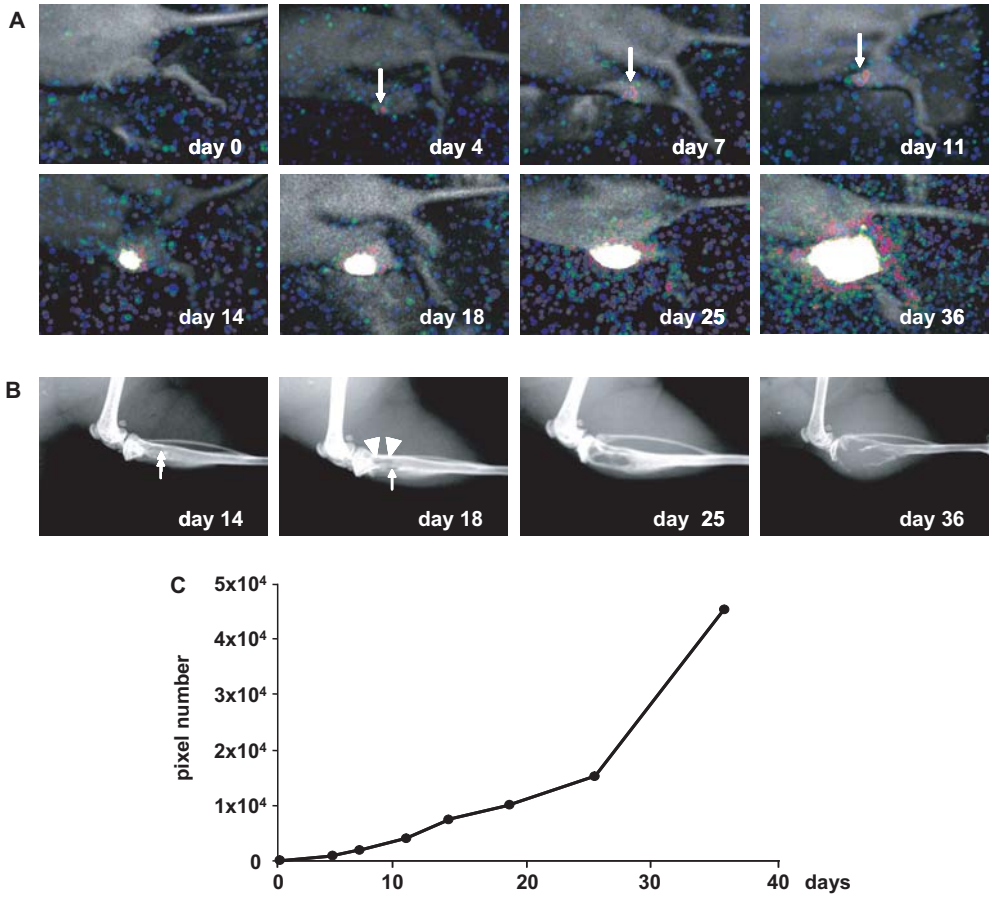


**Figure 6** **BLI and radiographic monitoring in vivo the growth kinetics of 2 x $10^4$ MDA-231-B/Luc+ cells implanted in the marrow cavity of the right tibia.** *A*, bioluminescent photon emission was recorded immediately (day 0) and at various time points in the 5 weeks following implantation. Signals are displayed as pseudo-color image at the most sensitive 0-3 bit range. Arrow at day 4, 7 and 11 highlights the initial photon accumulation over the area of implantation. *B*, radiographs of the corresponding tibia starting from day 14. Small arrow at day 14 and 18 points at the cortical hole that results from surgical drilling. Arrowheads at day 18 highlight the initial area of osteolysis. *C*, Growth curve obtained by quantification of the bioluminescent signal over the area of implantation during the 5-week recording period.

## Determination of the lowest cell number detectable in bone by BLI

Soon after direct inoculation of MDA-231-B/Luc+ cells into the marrow cavity of the femur, BLI could detect a signal from a number of cells as low as 2 x $10^4$. However, 1 x $10^4$ and 0.1 x $10^4$ cells could be detected if injected i.m. and s.c., respectively (not shown). Similarly, microscopic foci of spontaneous bone metastasis could easily be detected. In the specific case shown in figure 5 (*B* and *D*) the three major diameters of the metastatic lesion and the

density of the cancer cells were determined in serial sections comprehensive of the entire extension of the metastatic lesion. Assuming an ellipsoid shape, the total volume of the metastatic lesion resulted of ≈ 0.5 $mm^3$ volume and the total number of cells contained in it was calculated as ≈ 1.7 x $10^4$.

## Discussion

This investigation shows for the first time that the i.c. injection of MDA-231-B/Luc+ cancer cells combined to BLI is an ideal model for minimal residual disease (MRD), due to the remarkable sensitivity of the optical imaging in detecting microscopic bone marrow metastases *in vivo*.

The fate of the MDA-231-B/Luc+ cells could already be monitored by BLI immediately following intracardiac injection. The diffuse photon signal imaged over the entire animal body 10 minutes after injection was likely to be emitted by cancer cells not yet extravasated, and the areas of denser emission reflected presumably organs with the highest blood flow. The absence of signal 24 hours later conforms to the already reported rapid clearance and elimination of the majority of i.c. injected cancer cells [23]. Consistently with the elective bone /bone marrow tropism of the parental clone MDA-231-B, the same animal developed exclusively bone metastases within 4 weeks from i.c. injection of MDA-231-B/Luc+ cells. These findings further support the concept that organ specificity of metastases is not due to differences in blood perfusion, but largely depends on local interactions between cancer cells and the organ specific microenvironment [24].

All mice i.c. inoculated with the MDA-231-B sub-clone showed bone metastases, while only 1/4 of them showed soft tissue metastases, as detected by BLI. Thus the MDA-231-B possesses a higher bone-seeking capacity than the parental MDA-231 cell line, shown to induce bone metastases with lower incidence, but with a two-fold higher potential to metastasize to soft tissues [20]. This modified profile of organ distribution of metastases resembles very closely that already reported for another MDA-231 subclone similarly derived from a bone metastasis [25]. In contrast, none of the animals injected intravenously with the MDA-231-B sub-clone did develop either bone or soft tissue metastases. This seems to indicate that the cells are completely cleared by the lung already during the first passage through its circulation, further supporting the rationale for the intracardiac inoculation, as stated in the original description of the method [11]. The absence of metastatic growth in the lung after i.v. injection and the remarkable potential to metastasize to bone marrow after i.c. inoculation may suggest that the MDA-231-B sub-clone has acquired a growth advantage specific for the bone marrow microenvironment. Bone metastases induced by parental MDA-231 cells, when compared to brain and lung metastases, show increased expression of parathyroid hormone-related protein (PTH-rP) [20,25], macrophage colony stimulating factor (M-CSF) and vascular endothelial growth factor (VEGF) –A, -B and –C [20]. All these are

bone-resorbing or angiogenic cytokines and they may represent the molecular basis for the enhanced osteotropism of bone-seeking clones derived from cancer cell lines [20,25,26].

When compared to the conventional radiographic detection of osteolytic and/or osteosclerotic lesions, BLI offers the important advantage of detecting tumor growth in the marrow cavity much before development of radiologically evident osteolytic and/or osteosclerotic lesions. The early detection is explained by the fact that BLI detects directly tumor burden long before it reaches a critical size able to induce modifications of the local bone remodeling relevant enough to be recognized by radiography. As a consequence, the number of metastatic sites detected by BLI largely exceeds those identified by conventional radiography. It derives a gain in statistical significance and a reduction in the number of animals needed for each experimental group.

Radiography could not detect in any of the animals an osteolytic lesion that did not show also bioluminescent activity. Furthermore, a decline of bioluminescent activity of already developed metastases was never observed. Taken together, these observations indicate that luciferase expression *in vivo*, under non-selective conditions, was stable over the entire experimental period.

BLI could easily image *in vivo* a bone metastatic lesion that at the end-point histological analysis resulted in a tumor of ≈0.5 $mm^3$ volume, corresponding to ≈1.7x$10^4$ cells. A similar number of cells could be detected when inoculated directly into the bone marrow cavity. Considering that during the time elapsed between first detection (day 33 after i.c injection of cancer cells) and analysis *ex vivo* (day 38) the spontaneous metastatic lesion has grown, it is likely that BLI can detect bone metastatic growth of even smaller size. Nevertheless, BLI could detect a discrete signal from 1x $10^4$ and 0.1x $10^4$ cancer cells implanted i.m and s.c., respectively, clearly indicating that intensity of the signal detected by BLI is a function of the tissue composition and depth of the bioluminescent source. This is possibly due to light scattering and quenching by tissue components such as hemoglobin[16,27].

Polymerase chain reaction- (PCR-) based methods also allow sensitive detection and quantification of cancer cell burden in bone/bone marrow [20,28,29]. However, being methods *ex vivo*, they have severe limitations. First, in temporal studies several animal groups need to be sacrificed at different time points. Second, the bone sample is randomly selected and its size necessarily small and inevitably subject to sampling bias. Thus, large numbers of animals per group are needed to reach statistical significance. Third, these methods require disruption of the tissue samples. This precludes the possibility to perform parallel histology-based and gene expression analyses on the same bone sample. In contrast, BLI allows detailed anatomical information, continuous monitoring and precise quantification of bone metastatic growth *in vivo*, consistent reduction in the number of experimental animals and opportunity to perform end-point histological, immunohistological and gene expression analyses guided to the bone(s) specifically affected by metastatic disease.

A similar method of whole body reporter gene imaging able to visualize *in vivo* experimental metastases to bone and soft tissues has been reported [17]. This method utilizes GFP, instead of luciferase, as reporter gene. A possible concern regarding the use of GFP as reporter gene in whole body imaging is the auto-fluorescence generated in animal tissues by external light excitation [16,17]. This background fluorescence may decrease the sensitivity of detection and, thus, delay early identification of bone metastatic foci. The GFP-based whole body imaging could visualize a bone metastatic lesion of about 0.96 mm in diameter at best [17]. At this tumor size the cancer cells may have already induced osteolytic and/or osteosclerotic lesions sufficient to be recognized by radiography. However, the sensitivity of GFP-reporter external imaging was not compared to radiography, and no histological proof of the presence and histomorphometric measurement of the size of the bone metastases were given [17].

All carcinomas, both primary and secondary, when they reach the size of 2-3 $mm^3$ depend on angiogenesis for further growth [14,15]. The ability of BLI to detect externally bone metastatic foci of even smaller size is extremely relevant in view of the necessity to investigate the pre- and peri-angiogenic phases of metastatic growth.

The model of i.c. injection of *Luc*-transfected cancer cells coupled to BLI detection and continuous monitoring *in vivo* of bone metastases will facilitate studies on the molecular mechanisms involved in early stages of metastatic disease (MRD) and the development of innovative therapeutic strategies.

## Acknowledgments

We thank the Department of Clinical Research, University of Bern for the financial and logistic support. This work was supported by grants from the Swiss National Science Foundation Program 37 "Somatic Gene Therapy" (grant 4037-044804), Swiss National Science Foundation (grant 32-57118.99), CaPCURE, and "Stiftung zur Krebsbekämpfung".





## References

1. Boring CC, Squires TS, Tong T. Cancer statistics, 1993. *CA Cancer J Clin* 1993; 43:7-26.
2. Jaffe HL. Tumors metastatic to the skeleton. Tumors and tumorous conditions of the bone and joints. Edited by Jaffe HL. Philadelphia, Lea and Febiger, 1968, pp. 589-618.
3. Drew M, Dickinson RB. Osseous complications of malignancy. Clinical cancer medicine, treatment tactics. Edited by Lokich J. Boston, Hall, 1980, pp. 97-124.
4. Thalmann G, Anezinis P, Devoll R, Farach-Carson C, Chung LWK. Experimental approaches to skeletal metastasis of human prostate cancer. Principles and practices of genitourinary oncology. Edited by Raghavan D, Scher HI, Leibel SA, Lange PH. Philadelphia, Lippincott-Raven, 1997, pp 409-16.
5. Willis RA. The spread of tumors in the human body. London, Butterworth, 1973, pp. 229-250.
6. Braun S, Pantel K. Micrometastatic bone marrow involvement: detection and prognostic significance. *Med Oncol* 1999; 16:154-65.
7. McDonnell CO, Hill ADK, McNamara DA, Walsh TN, Bouchier-Hayes DJ. Tumor micrometastases: the influence of angiogenesis. *Eur J Surg Oncol* 2000; 26:105-15.

8. Hirsch-Ginsberg C: Detection of minimal residual disease: relevance for diagnosis and treatment of human malignancies. *Annu Rev Med* 1998; 49:111-122.
9. Kostler WJ, Brodowicz T, Hejna M, Wiltschke C, Zielinski CC. Detection of minimal residual disease in patients with cancer: a review of techniques, clinical implications, and emerging therapeutic consequences. *Cancer Detect Prev* 2000; 24:376-403.
10. Klein CA. The biology and analysis of single disseminated tumour cells. *Trends Cell Biol* 2000; 10:489-93.
11. Arguello F, Baggs RB, Frantz CN. A murine model of experimental metastasis to bone and bone marrow. Cancer Res 1988; 48:6876-81.
12. Yoneda T, Sasaki A, Mundy GR. Osteolytic bone disease in breast cancer. *Breast Cancer Res Treat* 1994; 32:73-84.
13. Yoneda T. Cellular and molecular basis of preferential metastasis of breast cancer to bone. *J Orthop Sci* 2000, 5:75-81.
14. Hanahan D, Folkman J. Patterns and emerging mechanisms of the angiogenic switch during tumorigenesis. *Cell* 1996, 86:353-364.
15. Carmeliet P, Jain RK. Angiogenesis in cancer and other diseases. *Nature* 2000; 407:249-257.
16. Contag CH, Jenkins D, Contag PR, Negrin RS. Use of reporter genes for optical measurements of neoplastic disease in vivo. *Neoplasia* 2000; 2:41-2.
17. Yang M, Baranov E, Jiang P, Sun FX, Li XM, Li L *et al.* Whole-body optical imaging of green fluorescent protein-expressing tumors and metastases. *Proc Natl Acad Sci USA* 2000; 97:1206-11.
18. Edinger M, Sweeny TJ, Tucker AA, Olomu AB, Negrin RS, Contag CH. Noninvasive assessment of tumor cell proliferation in animal models. *Neoplasia* 1999; 1:303-310.
19. Cailleau R, Yong R. Olive M, Reeves WJ. Breast tumor cell lines from pleural effusions. *J Natl Cancer Inst* 1974; 53:661-74.
20. van der Pluijm G, Sijmons B, Vloedgraven H, Deckers M, Papapoulos SE, Löwik CWGM. Monitoring metastatic behavior of human tumor cells in mice with species-specific polymerase chain reaction: elevated expression of angiogenesis and bone resorption stimulators by breast cancer in bone metastases. *J Bone Miner Res* 2001; 16:1077-91.
21. Nordeen SK. Luciferase reporter gene vectors for analysis of promoters and enhancers. *Biotechniques* 1988; 6:454-58.
22. Wang CW, Chang YW. A model for osseous metastasis of human breast cancer established by intrafemur injection of MDA-MB-435 cells in nude mice. *Anticancer Res* 1997; 17:2471-74.
23. Basse P, Hokland P, Heron I, Hokland M. Fate of tumor cells injected into the left ventricle of heart in Balb/c mice: role of natural killer cells. *J Natl Cancer Inst* 1988; 80:657-65.
24. Fidler IJ. Critical determinants of cancer metastasis: rationale for therapy. *Cancer Chemother Pharmacol* 1999, 43:S3-S10.
25. Yoneda T, Williams PJ, Hiraga T, Niewolna M, Nishimura R: A bone-seeking clone exhibits different biological properties from the MDA-MB-231 parental human breast cancer cells and a brain-seeking clone in vivo and in vitro. *J Bone Miner Res* 2001; 16:1486-95.
26. Koeneman KS, Yeung F, Chung LWK. Osteomimetic properties of prostate cancer cells: a hypothesis supporting the predilection of prostate cancer metastasis and growth in the bone environment. *Prostate* 1999; 39:246-61.
27. Colin M. Haemoglobin interferes with the ex vivo luciferase luminescence assay: consequence for detection of luciferase reporter gene expression *in vivo*. *Gene Ther* 2000; 7:1333-6.
28. Negrin RS, Blume KG. The use of the polymerase chain reaction for the detection of minimal residual disease. *Blood* 1991; 78: 255-8.
29. Sung V, Cattell DA, Bueno JM, Murray A, Zwiebel JA, Aaron AD, Thompson EW. Human breast cancer cell metastasis to long bone and soft organs of nude mice: a quantitative assay. *Clin Exp Metastasis* 1997; 15: 173-83.